ELSEVIER

Thermochimica Acta 386 (2002) 59–64

thermochimica acta

www.elsevier.com/locate/tca

Thermal characteristics of fatty acid copper(II) carboxylate complexes with nicotinamide and diethylnicotinamide ligands

S. Petriček*, B. Kozlevčar

Faculty of Chemistry and Chemical Technology, University of Ljubljana, Aškerčeva 5, P.O. Box 537, SI-1001 Ljubljana, Slovenia

Received 15 June 2001; received in revised form 27 August 2001; accepted 3 September 2001

Abstract

TG and DTA studies of $[Cu_2(OOCC_nH_{2n+1})_4(nia)_2]$ (nia = nicotinamide; $n = 6-11$) and $[Cu_2(OOCC_nH_{2n+1})_4(Et_2nia)_2]$ ($Et_2nia = N,N$-diethylnicotinamide; $n = 6-11$) are reported. The influence of the ligands in these complexes on the solid-to-liquid crystalline phase transition is established. Solid-to-solid, solid-to-liquid crystalline and liquid crystalline-to-isotropic liquid phase transitions are confirmed for the compounds with nia ligand $[(Cu_2(OOCC_nH_{2n+1})_4(nia)_2]$ ($n = 10, 11$) by variable temperature X-ray diffraction analysis and polarized optical microscopy. Only melting points are detected in all complexes with the Et_2nia ligand.

Keywords: Copper(II) carboxylates; Nicotinamide; Diethylnicotinamide; Liquid crystals; Thermal analysis; Variable temperature X-ray diffraction

1. Introduction

Solid-to-liquid crystal phase transitions occur in some copper(II) carboxylates in the temperature interval between 358 and 393 K [1–4]. These compounds consist of centrosymmetric tetracarboxylate-bridged dimers, $[Cu_2(OOCC_nH_{2n+1})_4]$ as reported for copper(II) decanoate [5], octanoate [6], heptanoate [7] and hexanoate [8]. Significant inter-dimer associations through copper and oxygen atoms in apical positions of adjacent dimers, as shown in Fig. 1, are typical for the simple copper(II) carboxylates [7,8]. The dimers are connected in chains, building an extended polymeric structure.

The complexes of nia ligand, $[Cu_2(OOCC_nH_{2n+1})_4(nia)_2]$ ($n = 6$ (**A**, **B**), 7, 8) [9,10] and Et_2nia, $[Cu_2(OOCC_7H_{15})_4(Et_2nia)_2]$ [11], crystallize in a dimeric form similar to $[Cu_2(OOCC_nH_{2n+1})_4]$, but dimer association is different due to ligands in the apical positions. The ligands nia and Et_2nia are coordinated to the apical positions through nitrogen atoms as for pyridine in $[Cu_2(OOCC_nH_{2n+1})_4(py)_2]$ ($n = 6-11$) complexes [12]. Similar structures were proposed for the other $[Cu_2(OOCC_nH_{2n+1})_4(nia)_2]$ ($n = 9-11$) and $[Cu_2(OOCC_nH_{2n+1})_4(Et_2nia)_2]$ ($n = 6$, 8–11) complexes according to the UV–Vis, IR, EPR spectra and magnetic measurements [9,11]. Dimers, connected to an extended sheet by hydrogen bonds, are characteristic only for nia series [9,10], but not for Et_2nia [11] series of compounds. Two different hydrogen bonding schemes are characteristic for **A** and **B** polymorphic forms of $[Cu_2(OOCC_6H_{13})_4(nia)_2]$. Hydrogen bonds N–H···O are formed in **B** form heptanoate similar as in nia octanoate and nonanoate from amide nitrogen to the amide and carboxylate oxygen atoms of adjacent dimers. Only amide–amide

* Corresponding author. Tel.: +386-1-241-91-20; fax: +386-1-241-92-20.
E-mail address: sasa.petricek@uni-lj.si (S. Petriček).

0040-6031/02/$ – see front matter
PII: S0040-6031(01)00758-4

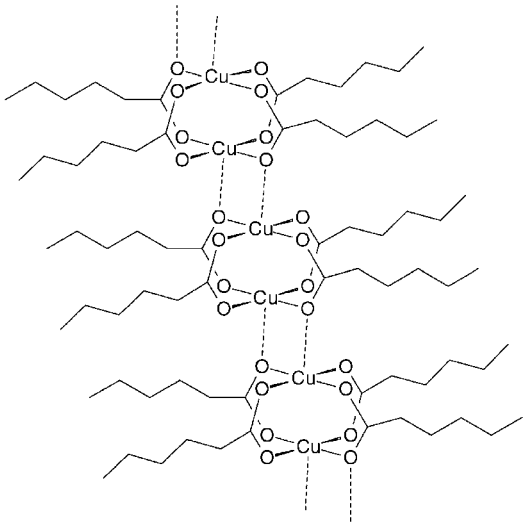

Fig. 1. Inter-dimer associations through copper and oxygen atoms in apical positions of adjacent dimers.

hydrogen bonds are present in **A** form of nia heptanoate, resulting in a honeycomb-like network [9]. Ethyl groups replace hydrogen atoms in the complexes of $[Cu_2(OOCC_nH_{2n+1})_4(Et_2nia)_2]$ and prevent association to a network through hydrogen bonds.

Phase transitions of copper(II) carboxylates with nitrogen donor ligands have been reported for pyridine complexes $[Cu_2(OOCC_nH_{2n+1})_4(py)_2]$ $(n = 8, 9, 11)$ [13] and for a pyridine derivative, dodecylnicotinate complexes, in $[Cu_2(OOCC_nH_{2n+1})_4(C_5H_4NCOOC_{12}H_{25})_2]$ $(n = 10, 12, 14, 16, 18, 20)$ [14]. We have studied the thermal behavior of the copper(II) carboxylate complexes with nia and Et_2nia. DTA and TG curves of these complexes have been recorded to determine whether a transition to a liquid crystalline phase takes place on heating. The transition to a liquid crystalline phase on heating was confirmed by variable temperature X-ray diffraction studies and polarized microscopy. The explanation of different thermal characteristics in the complexes $[Cu_2(OOCC_n\ H_{2n+1})_4(L)_2]$ $(L = nia, Et_2nia)$ is presented.

2. Experimental

2.1. Materials

The complexes of $[Cu_2(OOCC_nH_{2n+1})_4(nia)_2]$ $(n = 6-11)$ [9] and $[Cu_2(OOCC_nH_{2n+1})_4(Et_2nia)_2]$ $(n = 6-11)$ were prepared as reported previously [11].

2.2. Physical measurements

Simultaneous TG and DTA measurements were made on a Mettler TA 2000 under 99.999% pure argon with the flow rate of 35 ml min^{-1}. The reference material Al_2O_3 was employed in all experiments. The first measurement for each compound was done at a heating rate of 2 K min^{-1} up to 773 K in order to determine the solid–mesophase and mesophase–isotropic liquid transition temperatures. The subsequent measurements were performed at a heating rate of 1 K min^{-1}, some of them with consequent cooling and repeated heating to check reversibility of phase transitions. The temperature and energy corrections were done by melting of indium (429.6 K) and zinc (692.6 K). Repeated measurements have shown uncertainties in the temperature range of ± 1 K and $\pm 10\%$ kJ mol^{-1}. The noise in DTA curves is negligible in the applied temperature range, being less than 2% of observed peaks.

X-ray powder diffraction patterns of samples before and after thermal treatment were recorded on a Huber Guinier camera.

Variable temperature X-ray diffraction patterns were collected on Siemens D-5000 diffractometer, with a HTK-16 high temperature chamber using Cu Kα radiation. The compounds were heated in air at 5 K min^{-1} to the starting temperature, which was than held until the end of scanning. The samples were scanned in the 2Θ range between 4° and 20° in steps of 0.026° 2Θ and an integration time of 4 s per step.

Polarized microscopy. Specimen temperature was regulated with a programmed control system Mettler Toledo FP82, capable of multiple heating/cooling ramps at various rates. The microscopy studies were conducted with a Carl Zeiss STEMI SV6 microscope. Birefringence was observed using two Zeiss plane-polarizing filters oriented as fully-crossed polars.

3. Results and discussion

3.1. $[Cu_2(OOCC_nH_{2n+1})_4(Et_2nia)_2]$ $(n = 6–11)$

Et_2nia complexes, $[Cu_2(OOCC_nH_{2n+1})_4(Et_2nia)_2]$ $(n = 6-11)$, decompose above 413 K. Decomposition

Table 1
Melting points of $[Cu_2(OOCC_nH_{2n+1})_4(Et_2nia)_2]$ and $[Cu_2(OOCC_nH_{2n+1})_4(nia)_2]$ phase transition temperatures for $[Cu_2(OOCC_nH_{2n+1})_4(nia)_2]$ compounds and corresponding enthalpies determined from DTA curves

n	$[Cu_2(OOCC_nH_{2n+1})_4(Et_2nia)_2]$, T_{melt} (K) (measured, ±1 K)	$[Cu_2(OOCC_nH_{2n+1})_4(nia)_2]$		$[Cu_2(OOCC_nH_{2n+1})_4(nia)_2]$, ΔH_{trans} (kJ mol^{-1}) (measured, ±10%)
		T_{trans} (K) (measured, ±1 K)	T_{melt} (K) (measured, ±1 K)	
6	324	–	449[a,b]	
7	–	–	455[a]	
8	327	411[c]	451[a]	8.5[c]
9	328	–	438[a]	
10	329	378[c], 413[d]	429	22[c], 23[d]
11	338	366[c], 395[d]	432	5.8[c], 32[d]

[a] Melting and decomposition occur in the same temperature range.
[b] Melting points of both heptanoate nia complexes are equal.
[c] Temperature of a solid-to-solid transition.
[d] Temperature of a solid-to-liquid crystalline phase transition.

products consist of copper(I), copper(II) oxides and copper according to the X-ray diffraction patterns recorded after thermal treatments to 773 K. A sharp endothermic peak appears in the DTA curves of Et_2nia series of complexes in the temperature range from 324 to 338 K (Table 1). The samples were studied also under the microscope during heating from room temperature to 350 K. The observation under the microscope confirmed that all investigated Et_2nia complexes melt directly to an isotropic liquid in the temperature range from 324 to 338 K. Direct transformation from solid to isotropic liquid was observed also in the dodecylnicotinate complexes [14]. Hydrogen bonding is not possible in neither of these two series of compounds, $[Cu_2(OOCC_nH_{2n+1})_4(C_5H_4NCOOC_{12}H_{25})_2]$ [14] or $[Cu_2(OOCC_nH_{2n+1})_4(Et_2nia)_2]$. The melting points of the complexes with Et_2nia increase with an increasing number of carbon atoms in aliphatic chains, but significantly higher melting points were determined for nia complexes due to hydrogen bonds, which are formed in $[Cu_2(OOCC_nH_{2n+1})_4(nia)_2]$ (Table 1).

3.2. $[Cu_2(OOCC_nH_{2n+1})_4(nia)_2]$ ($n = 6$–11)

Phase transitions of the investigated nia complexes are shown in Fig. 2. Representative DTA and TG curves of $[Cu_2(OOCC_{11}H_{23})_4(nia)_2]$ (DTA12) and $[Cu_2(OOCC_6H_{13})_4(nia)_2]$ form **B** (DTA7, TG7) are shown in Fig. 3. Endothermic peaks in the DTA curve prior to melting were observed only for the complexes

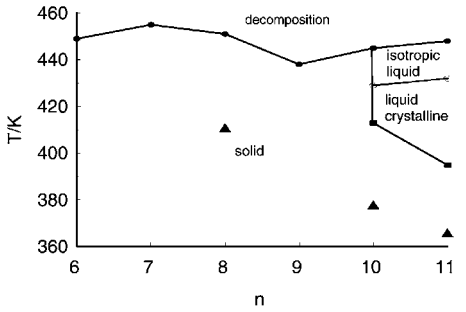

Fig. 2. Phase transitions of $[Cu_2(OOCC_nH_{2n+1})_4(nia)_2]$ complexes, where $n = 6$–11: (●) temperature of decomposition, (○) temperature of liquid crystalline-to-isotropic liquid transition (■) temperature of solid-to-liquid crystalline phase transition, (▲) temperature of solid-to-solid phase transition.

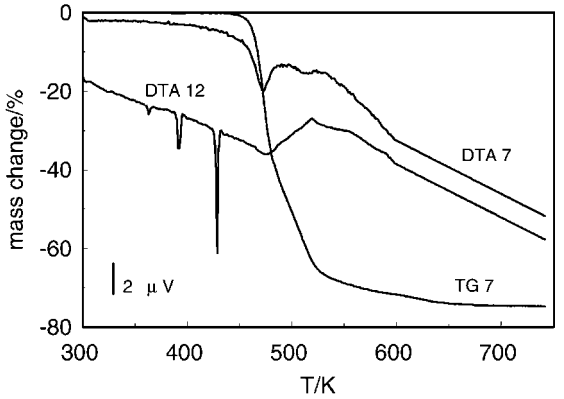

Fig. 3. TG and DTA curves for $[Cu_2(OOCC_6H_{13})_4(nia)_2]$ form **B** (TG7 and DTA7) and $[Cu_2(OOCC_{11}H_{23})_4(nia)_2]$ (DTA12).

with longer paraffin chains like $[Cu_2(OOCC_nH_{2n+1})_4(nia)_2]$ ($n = 8, 10, 11$), but not for $[Cu_2(OOCC_nH_{2n+1})_4(nia)_2]$ ($n = 6$, **A** or **B**, 7, 9). One endothermic peak appeared in the DTA curve of nia nonanoate and two in the DTA curves of nia undecanoate and dodecanoate. The temperatures of the phase transitions and the corresponding enthalpy changes, as determined from DTA measurements, are presented in Table 1. Thermal decomposition of the solid $[Cu_2(OOCC_nH_{2n+1})_4(nia)_2]$ ($n = 6-9$) begins at the same temperature as melting, while $[Cu_2(OOCC_nH_{2n+1})_4(nia)_2]$ ($n = 10, 11$) decompose approximately 15 K above the corresponding melting points.

Variable temperature XRD and polarized microscopy were used to determine the nature of the observed phase transitions in $[Cu_2(OOCC_nH_{2n+1})_4(nia)_2]$ ($n = 8, 10, 11$). The XRD pattern of a liquid crystalline phase is dominated by a relatively intense peak at an angle below 10° in 2Θ [15]. Liquid crystal transition temperatures of $[Cu_2(OOCC_nH_{2n+1})_4]$ ($n = 3-24$) and the results of variable temperature XRD have been published in the literature [2,4]. We have compared the variable temperature XRD patterns of $[Cu_2(OOCC_nH_{2n+1})_4]$ ($n = 5, 6$) and $[Cu_2(OOCC_nH_{2n+1})_4(nia)_2]$ ($n = 8, 10$). The characteristic peaks in the XRD pattern for the solid $[Cu_2(OOCC_6H_{13})_4]$ disappeared at 373 K, because the solid $[Cu_2(OOCC_6H_{13})_4]$ transforms at 370 K to a mesophase. Only a dominant peak at the angle 6.65° ($d_1 = 13.3$ Å) and a broad peak of low intensity at value approximately to $d_1/3^{1/2}$ ($d_2 = 7.69$ Å) were observed at 373 K. Similar results were obtained for $[Cu_2(OOCC_5H_{11})_4]$, but the intense peak appeared at a lower d value ($d_1 = 12.4$ Å). Decreasing of d_1 values in the XRD patterns of the mesophases for the complexes with shorter aliphatic chains were also observed in the previous investigations [2,4,15]. The d_1 values in $[Cu_2(OOCC_nH_{2n+1})_4]$ ($n = 5, 6$) are between the values of the longest axes in the triclinic unit cells [7,8], which is also characteristic for $[Mo_2(OOCC_nH_{2n+1})_4]$ [15].

The XRD patterns obtained for two nia complexes, $[Cu_2(OOCC_8H_{17})_4(nia)_2]$ and $[Cu_2(OOCC_{10}H_{21})_4(nia)_2]$, are presented in Figs. 4 and 5. Only a solid-to-solid transition, as suggested by DTA and observation under the microscope, is confirmed for nonanoate. On the other hand, two different phase transitions,

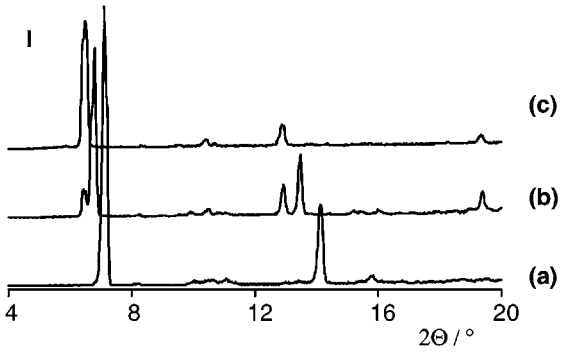

Fig. 4. Variable temperature XRD of $[Cu_2(OOCC_8H_{17})_4(nia)_2]$: (a) the low temperature solid phase at 298 K; (b) a mixture of the low and high temperature solid phases at 403 K; (c) the high temperature solid phase at 413 K.

solid-to-solid and solid-to-liquid crystal were confirmed for undecanoate by the results of variable temperature XRD. The first endothermic peak at 378 K in the DTA curve of $[Cu_2(OOCC_{10}H_{21})_4(nia)_2]$ corresponds to a solid-to-solid transition. The high temperature form transforms at 413 K to the liquid crystalline phase, as seen in Fig. 5(c). This is in accordance to the second endothermic peak in the DTA curve (Table 1). The dominant peak in the XRD pattern of the liquid crystalline phase appeared at the

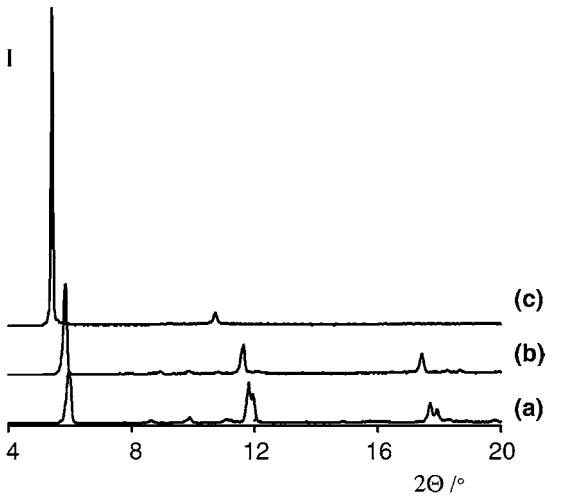

Fig. 5. Variable temperature XRD of $[Cu_2(OOCC_{10}H_{21})_4(nia)_2]$: (a) the low temperature solid phase at 298 K; (b) the high temperature solid phase at 383 K; (c) the liquid crystalline phase at 413 K.

angle 5.40° in 2Θ ($d_1 = 16.4$ Å) and the broad peak of low intensity at $d_2 = 8.26$ Å (approximately $d_1/2$). The appearance of weak peaks at values of approximately $d_1/3^{1/2}$ and $d_1/2$ indicate similar discotic mesophases in $[Cu_2(OOCC_nH_{2n+1})_4]$ ($n = 5, 6$) and $[Cu_2(OOCC_{10}H_{21})_4(nia)_2]$ as in $[Mo_2(OOCC_nH_{2n+1})_4]$ [15]. We propose relatively ordered mesophases in $[Cu_2(OOCC_nH_{2n+1})_4(nia)_2]$ ($n = 10, 11$) due to the intense endothermic peaks in DTA curves for formation of isotropic liquid (Fig. 3, DTA12).

Only a bursting of the surface was observed during heating of $[Cu_2(OOCC_nH_{2n+1})_4(nia)_2]$ ($n = 8, 10, 11$) under the polarizing microscope at the temperatures corresponding to the first endothermic effect in the DTA curves. Upon cooling from the isotropic liquid $[Cu_2(OOCC_nH_{2n+1})_4(nia)_2]$ ($n = 10, 11$) complexes display fan-shaped optical textures, which are typical for discotic mesophases [15]. The results of thermal analysis, variable temperature XRD and polarized microscopy verify that the peaks in the DTA curves at lower temperatures represent a solid-to-solid phase transition for $[Cu_2(OOCC_nH_{2n+1})_4(nia)_2]$ (8, 10, 11) and a solid-to-liquid crystalline phase transition at higher temperatures for undecanoate and dodecanoate (Fig. 2).

Repeated heating to 420 K with subsequent cooling was undertaken for compounds $[Cu_2(OOCC_nH_{2n+1})_4(nia)_2]$ ($n = 8, 10, 11$). The phase changes are reversible as shown in Fig. 6 for nia dodecanoate complexes. DTA curves obtained during heating were practically unchanged even after several heating–cooling cycles. The inverse transition from the liquid crystalline phase to the solid phase occurs almost at the same temperatures. The solid-to-solid phase transition takes place in both compounds upon cooling at temperatures which are 10–20 K lower than the transition temperatures on heating.

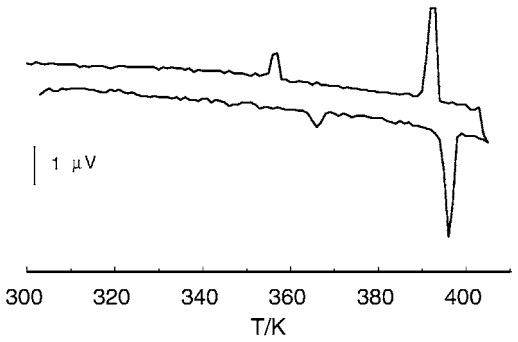

Fig. 6. DTA curve for a repeated heating and cooling of $[Cu_2(OOCC_{11}H_{23})_4(nia)_2]$ revealed the reversibility of the phase transitions.

A solid-to-solid phase transition can be explained in undecanoate and dodecanoate nia complexes similar to that for dodecylnicotinate complexes [14] by significant changes in inter-chain interactions between long, almost parallel, alkyl chains of neighboring dimers at transition temperatures. The explanation for a solid-to-solid phase transition in nia nonanoate complex with shorter alkyl chains may be different. For nonanoate nia complex, a non-symmetric arrangement of alkyl chains is characteristic at room temperature, while other complexes display a centrosymmetric tetracarboxylates arrangement. The reason for the phase transition in the nia nonanoate complex may be rearrangement of nonanoate chains in dimers at the transition temperature.

Transition from a liquid crystalline phase into an isotropic liquid occurs in $[Cu_2(OOCC_nH_{2n+1})_4(nia)_2]$ ($n = 10, 11$) above 429 K, shortly before decomposition (Fig. 2).

The formation of liquid crystalline phase occurs in these two nia complexes at temperatures which are 15–28 K higher than in corresponding $[Cu_2(OOCC_nH_{2n+1})_4]$. Melting and decomposition of the nia complexes begin at temperatures which are approximately 60 K lower than in $[Cu_2(OOCC_nH_{2n+1})_4]$ [13].

A similar influence of the paraffin chain length on liquid crystal formation as in $[Cu_2(OOCC_nH_{2n+1})_4(nia)_2]$ was described for $[Cu_2(OOCC_nH_{2n+1})_4(py)_2]$ [13]. A liquid crystalline phase appeared only in the complexes with longer alkyl chains, $n \geq 8$ in complexes of pyridine and $n \geq 10$ in nia complexes. A significant association through copper and oxygen atoms in adjacent dimers which plays an important role in thermal behavior and mesophase formation of low fatty acid complexes $[Cu_2(OOCC_nH_{2n+1})_4]$ [4] is not possible in complexes with nia or pyridine. A formation of liquid crystalline phase was observed only in $[Cu_2(OOCC_nH_{2n+1})_4(nia)_2]$ ($n = 10, 11$), when ordering of aliphatic chains becomes an important factor as in $[Cu_2(OOCC_nH_{2n+1})_4]$ [4]. The temperature range of mesophase increases from undecanoate to dodecanoate nia complex.

4. Conclusion

Solid-to-liquid crystalline phase transitions were observed in some copper(II) carboxylates with a significant inter-dimer association to a network. Dimers in the compounds $[Cu_2(OOCC_nH_{2n+1})_4(nia)_2]$ are connected via hydrogen bonds. A mesophase appears only in $[Cu_2(OOCC_nH_{2n+1})_4(nia)_2]$ complexes with longer paraffin chains ($n = 10, 11$). Et_2nia disables hydrogen bonding and connection of $[Cu_2(OOCC_nH_{2n+1})_4(Et_2nia)_2]$ dimers, consequently, only melting at lower temperatures was observed. The undecanoate and dodecanoate nia compounds showed a solid-to-solid transition prior to a solid–mesophase transition. These two transitions are reversible. Some distinctive differences were observed comparing the thermal behavior of copper(II) carboxylates, $[Cu_2(OOCC_nH_{2n+1})_4]$, to corresponding nia complexes. The transition temperatures for the formation of liquid crystalline phases in nia compounds are higher (nia undecanoate 413 K, nia dodecanoate 395 K) than in copper(II) carboxylates (undecanoate 383 K, dodecanoate 380 K). The temperature range of the mesophase is narrow, 16–37 K, in $[Cu_2(OOCC_nH_{2n+1})_4(nia)_2]$ ($n = 10, 11$) and wide, approximately 100 K, in $[Cu_2(OOCC_nH_{2n+1})_4]$. A liquid crystal–isotropic liquid transformation was observed only in $[Cu_2(OOCC_nH_{2n+1})_4(nia)_2]$ ($n = 10, 11$), while melting and decomposition take place in $[Cu_2(OOCC_nH_{2n+1})_4]$ simultaneously.

Acknowledgements

The financial support of the Ministry of Education, Science and Sport, Republic of Slovenia, through grant PS-511-103-01 is gratefully acknowledged. We thank Prof. P. Šegedin and Prof. A. Meden for helpful discussions, Prof. V. Kaučič from the National Institute of Chemistry, Slovenia for X-ray powder diffraction data and Mr. E. Kranjc for technical assistance.

References

[1] H.D. Burrows, H.A. Ellis, Thermochim. Acta 52 (1982) 121.
[2] H. Abied, D. Guillon, A. Skoulios, P. Weber, A.M. Giroud-Godquin, J.C. Marchon, Liquid Cryst. 2 (1987) 269.
[3] H. Abied, D. Guillon, A. Skoulios, A.M. Giroud-Godquin, P. Maldivi, J.C. Marchon, Colloid Polym. Sci. 266 (1988) 579.
[4] M. Ibn-Elhaj, D. Guillon, A. Skoulios, A.M. Giroud-Godquin, P. Maldivi, Liquid Cryst. 11 (1992) 731.
[5] T.R. Lomer, K. Perera, Acta Cryst. B 30 (1974) 2913.
[6] T.R. Lomer, K. Perera, Acta Cryst. B 30 (1974) 2912.
[7] N.E. Ghermani, C. Lecomte, C. Rapin, P. Steinmetz, B. Malaman, Acta Cryst. B 50 (1994) 157.
[8] A. Doyle, J. Felcman, M.T. do Prado Gambardella, C.N. Verani, M.L. Bragança Tristão, Polyhedron 19 (2000) 2621.
[9] B. Kozlevčar, N. Lah, I. Leban, I. Turel, P. Šegedin, M. Petrič, F. Pohleven, A.J.P. White, D.J. Williams, G. Giester, Croat. Chem. Acta 72 (1999) 427.
[10] B. Kozlevčar, Ph.D. Thesis, University of Ljubljana, Slovenia, 1999.
[11] B. Kozlevčar, N. Lah, I. Leban, F. Pohleven, P. Šegedin, Croat. Chem. Acta 73 (2000) 733.
[12] M. Petrič, I. Leban, P. Šegedin, Polyhedron 12 (1993) 1973.
[13] S. Petriček, M. Petrič, Thermochim. Acta 302 (1997) 35.
[14] M. Rusjan, Z. Chaia, O.E. Piro, D. Guillon, F.D. Cukiernik, Acta Cryst. B 56 (2000) 666.
[15] D.V. Baxter, R.H. Cayton, M.H. Chisholm, J.C. Huffman, E.F. Putilina, S.L. Tagg, J.L. Wesemann, J.W. Zwanziger, F.D. Darrington, J. Am. Chem. Soc. 116 (1994) 4551.